

# A DISCONTINUOUS GALERKIN METHOD FOR COMPUTING TIME-OF-FLIGHT IN DISCRETE-FRACTURE MODELS

B. EIKEMO<sup>1</sup>, I. BERRE<sup>1</sup>, H.K. DAHLE<sup>1</sup>, K.-A. LIE<sup>2,3</sup>, AND J. R. NATVIG<sup>2</sup>

<sup>1</sup>Dept. Mathematics, University of Bergen, Johs. Brunsgt. 12, N-5008 Bergen, Norway

<sup>2</sup>SINTEF ICT, Applied Mathematics, P.O. Box 124 Blindern, N-0314 Oslo, Norway

<sup>3</sup>Centre of Mathematics for Applications (CMA), University of Oslo, Norway

## ABSTRACT

Discrete fracture models, in which fractures are represented individually as lower-dimensional objects, are beginning to appear in simulators for porous media flow. Here we present a discontinuous Galerkin method for computing time-of-flight in discrete-fracture models of fracture-fault systems. Isocontours of time-of-flight are time-lines of porous-media flow and give information about flow patterns, in particular for single-phase flow.

Recent numerical results show that the discontinuous Galerkin (dG) method is efficient and accurate for solving the time-of-flight equation. In this paper, we use two simplified grid models to examine various approaches for the dG discretisation in fractured regions of the porous medium. Comparing the numerical results of the dG approximation with those from a streamline simulator, we demonstrate the importance of a sufficient grid resolution across the fractures, even though the widths of the fractures are very small compared to typical length scales of the unfractured parts of the reservoir.

## 1. INTRODUCTION

In recent years, advanced drilling techniques and enhances in seismic and geological characterisation of petroleum reservoirs have emerged. Consequently, there is an increased need for more detailed understanding of how local reservoir heterogeneities, such as fractures, affect the oil and gas recovery. A naturally fractured reservoir can be defined as a reservoir containing planar discontinuities created by natural processes like diastrophism and volume shrinkage. Due to the complex geometries and potentially large variations in parameter values, fractures will often have a significant impact on the flow characteristics of a porous medium, and fractured reservoirs represent a challenge for reservoir characterisation, modelling, and simulation.

The traditional way of simulating flow in a fractured medium is by the use of dual-porosity models, where the matrix (unfractured rock) and fractures are treated as two co-existing porous media. Although such models are efficient in some cases, they generally fail to deliver sufficient resolution of the complex flow patterns that develop when a fractured medium is produced. In recent years, several approaches have been taken to describe fracture-fault systems more accurately. These approaches rely a discrete description of individual fractures, using complex (unstructured) gridding schemes in which each fracture is represented explicitly by lower-dimensional objects at cell faces.

In a recent paper (Natvig et al., 2006), we presented a discontinuous Galerkin (dG) method for computing single-phase transport in porous media. Here we present the first step towards extending this method to discrete fracture systems. For simplicity, we only consider conceptual 2D models consisting of a regular Cartesian grid representing the matrix and extra lines at cell edges representing straight fractures. The aim of this first step is to investigate how the dG discretisation is able to handle the geometries and sharp variations in rock properties of fractured fields. In general, we use the same solution procedure as in (Natvig et al., 2006), but due to the high contrasts and different length scales of the rock matrix and the fractures, we investigate different dG approximation strategies for the model equation in the fractures. A key point in our approach is an efficient solution procedure for the resulting system of discrete flow equations. By exploiting *a priori* knowledge of the directions of flow, we may arrange the elements in a suitable sequence such that one does not need to assemble the full system and can compute the solution extremely fast in an element-by-element fashion.

The outline of the paper is as follows: In Section 2, we introduce the time-of-flight formalism as a model for single-phase transport in porous media. In Section 3, we give a brief outline of the dG method and present the variational formulation and discretisation of our model problem, distinguishing between the discretisation in the rock matrix and in the fractures. We also show how to solve the resulting linear system using an a priori reordering of the elements. Numerical examples are presented in Section 4; here, we compare the accuracy of the solutions computed by the dG method to highly resolved solutions obtained by pointwise integration of streamlines. Finally, we draw some conclusions and indicate further work.

## 2. GOVERNING EQUATIONS

We consider single-phase transport in porous media. The velocity field  $\mathbf{v}$  is governed by Darcy's law, and for convenience we assume that  $\mathbf{v} = \mathbf{v}(\mathbf{x})$  is given and is nearly irrotational and divergence free. The motion of the fluid is aligned with the velocity field  $\mathbf{v}$ ; thus, all instantaneous transport occurs along integral curves (streamlines). A streamline  $\Psi$  is the path traced out by a passive particle moving with the flow given by a velocity field  $\mathbf{v}$  such that the vector  $\mathbf{v}$  is tangential to  $\Psi$  at every point. The time-of-flight  $\tau(x)$  is the time needed for a passive particle to travel along a streamline from the inflow boundary to a given point  $x$ . Isocontours of  $\tau(x)$  are the time-lines in the porous medium and give information about the flow patterns, in particular for single-phase flow. The time-of-flight can be defined by the following integral along a streamline  $\Psi$ :

$$\tau(x) = \int_{\Psi} \frac{\phi ds}{|\mathbf{v}(x(s))|}, \quad (1)$$

where  $\phi$  is the porosity of the porous medium. Hence, a simple model for convective transport in  $\mathbf{v}$  is the boundary-value problem for time-of-flight  $\tau$  in  $\Omega$ :

$$\mathbf{v} \cdot \nabla \tau = \phi, \quad \tau = 0 \text{ in } \partial\Omega^+; \quad (2)$$

see (Datta-Gupta and King, 1995). Here,  $\partial\Omega^+$  denotes the inflow boundary of the fluid. Accurate solution of (2) is rather easy for smooth velocities, but the equation becomes harder to solve when the vector field has large spatial variations and fine-scale details. In

this paper, we will show the efficiency and accuracy of the dG method to simulate single-phase transport in fractured porous media as described by (2); however, the solution strategy also applies for slightly more general models of the same type; see (Natvig et al., 2006). We refer to (Natvig and Lie, 2006) for an extension of the dG methodology in to multiphase and multicomponent flow.

### 3. DISCONTINUOUS GALERKIN METHOD

The physical domain  $\Omega$  consists of matrix and fractures. Since fractures exist on a much smaller geometrical scale than the characteristic length scale of the matrix, we assume that we have a discrete fracture model, where the fractures are modelled as one-dimensional curves in a two-dimensional reservoir model. However, for the numerical calculations, we let the fractures have a small width  $\epsilon$ , so that both the matrix and the fracture are two dimensional.

The domain is partitioned into a regular quadrilateral grid of  $N$  elements  $\{E_i\}_{i=1}^N$ . More precisely, we denote the  $M$  elements corresponding to the matrix by  $\{K_i\}_{i=1}^M$  and the  $N - M$  elements describing the fractures by  $\{I_i\}_{i=1}^{N-M}$ . As quadrilateral corner-point grids can be transformed to regular grids (Prévost et al., 2002), the method can be extended to also handle more general partitions.

In the following, we describe the discretisation of the time-of-flight equation (2) using a discontinuous Galerkin method (Reed and Hill, 1973), distinguishing between the discretisation in the matrix and in the fracture elements. Thereafter, we explain the numerical solution procedure. It is assumed that the fluid velocity  $\mathbf{v}$  is a time-independent function that is given in terms of fluxes across the element edges.

**3.1. Approximation in the Matrix.** Let  $V$  be the space of arbitrarily smooth test functions. By multiplying (2) with a function  $\varphi \in V$  and integrating by parts over each matrix element  $K$ , we obtain

$$-\int_K T\mathbf{v} \cdot \nabla\varphi \, d\mathbf{x} + \int_{\partial K} T\mathbf{v} \cdot \mathbf{n}\varphi \, ds = \int_K \phi\varphi \, d\mathbf{x} \quad \forall \varphi \in V, \quad (3)$$

where  $\mathbf{n}$  is the outer normal on the element boundary  $\partial K$ . We seek a solution in a finite-dimensional subspace  $V_h \subset V$ , so we replace the exact solution and the test function by  $T_h \in V_h$  and  $\varphi_h \in V_h$ , respectively. The space  $V_h$  consists of functions that are smooth inside each element, but may be discontinuous over the element boundaries. Since  $T_h$  may be discontinuous over the element boundaries, we must replace the flux term,  $T\mathbf{v} \cdot \mathbf{n}$ , by a consistent and conservative numerical flux function  $\hat{f}$ . This leads to the following discrete variational formulation: Find  $T_h$  such that

$$-\int_K (T_h\mathbf{v}) \cdot \nabla\varphi_h \, d\mathbf{x} + \int_{\partial K} \hat{f}(T_h, T_h^{ext}, \mathbf{v} \cdot \mathbf{n})\varphi_h \, ds = \int_K \phi\varphi_h \, d\mathbf{x} \quad \forall K, \quad \forall \varphi_h \in V_h. \quad (4)$$

For inner and outer approximations  $T_h$  and  $T_h^{ext}$  at the boundaries, the numerical flux  $\hat{f}$  is approximated by the upwind flux given by

$$\hat{f}(T_h, T_h^{ext}, \mathbf{v} \cdot \mathbf{n}) = T_h \max(\mathbf{v} \cdot \mathbf{n}, 0) + T_h^{ext} \min(\mathbf{v} \cdot \mathbf{n}, 0). \quad (5)$$

The upwind approximation of the flux preserves the directional dependency that we will later exploit to compute the solution element by element.

The restriction  $\varphi|_K$  of a function  $\varphi \in V_h$  on an element  $K$  is defined by  $\varphi|_K \in \mathbb{Q}^{n-1}$ , where  $\mathbb{Q}^n = \text{span}\{x^p y^q : 0 \leq p, q, \leq n\}$ . Hence, for  $n = 1$ ,  $V_h^{(1)}$  is the space of functions that are elementwise constant in the unfractured domain and yields a scheme that is formally first order; for  $n = 2$ ,  $V_h^{(2)}$  is the space of elementwise bilinear functions on the unfractured domain and yields a formally second order accurate scheme; and so on.

**3.2. Approximation in the Fractures.** Since it is assumed that the width  $\epsilon$  of the fractures is negligible compared to characteristic length scales of the reservoir, we first consider a modification of the discretisation described above for the fracture elements,  $\{I_i\}$ , by assuming that there is no variation in time-of-flight across the fracture. This is consistent with the initial reservoir model, which assumes that the fractures have zero width. Depending on the position of the fractures, the thin fracture elements  $\{I_i\}$  are placed in either the  $x_1$ -direction or the  $x_2$ -direction.

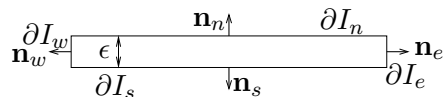


FIGURE 1. Fracture element of width  $\epsilon$ .

Assuming a constant solution across the fracture, and using the same framework as for the discretisation in the matrix, we obtain the following discrete variational formulation for a fracture element  $I_i$  placed in the  $x_1$ -direction: Find  $T_h$  such that for all  $\varphi_h \in V_h$

$$\begin{aligned}
 -\epsilon \int_{I_{x_1}} (T_h \mathbf{v}) \cdot \nabla \varphi \, dx_1 + \epsilon T_h \varphi_h \mathbf{v} \cdot \mathbf{n}_w + \int_{\partial I_s} T_h \varphi_h \mathbf{v} \cdot \mathbf{n}_s \, dx_1 \\
 + \epsilon T_h \varphi_h \mathbf{v} \cdot \mathbf{n}_e + \int_{\partial I_n} T_h \varphi_h \mathbf{v} \cdot \mathbf{n}_n \, dx_1 = \epsilon \int_{I_{x_1}} \varphi_h \, dx_1.
 \end{aligned} \tag{6}$$

For fracture elements located in the  $x_2$ -direction, a discretisation is obtained in the same manner, using that the solution is constant across the fractures in the  $x_1$ -direction. To compute the boundary integral we use the upwind flux function (5), where  $\mathbf{n}_w$ ,  $\mathbf{n}_s$ ,  $\mathbf{n}_e$ , and  $\mathbf{n}_n$  denote the outer normals at each element boundaries. Additionally, we use that  $\partial I = \partial I_w \cup \partial I_s \cup \partial I_e \cup \partial I_n$ ; see Figure 1. Since the order of the scheme is reduced to one in the direction across the fractures, the discretisation is simplified compared with the discretisation (4) in the matrix elements.

As an alternative, we may model the fractures as fully two-dimensional objects and approximate the solution in fracture elements in exactly the same manner as for the matrix elements. This can be motivated based on the fact that the flow changes rapidly in the fractured regions. For this reason, it is also natural to consider a finer grid resolution across the fracture (as opposed to only one element). The two alternative discretisations are discussed further in Section 4 by the means of two numerical examples. See (Hoteit and Firoozabadi, 2005) for a different dG approach.

**3.3. Numerical Solution Procedure.** The approximate solution and the test function on an element  $E_i$  can be written as a linear expansion of basis functions. By substituting this into the variational formulations (4) for the matrix elements and (6) for the fracture elements and approximating the integrals using Gaussian quadrature, we get a set of

linear equations for the degrees-of-freedom in each element. Let  $T_i$  denote the vector of unknowns for element  $E_i$ . If  $n$  denotes the order of the scheme, the number of unknowns per element using a dG method is  $n^2$  for matrix elements, and  $n$  for fracture elements if the order reduction in the dG approximation across the fractures is applied.

Let us now examine the structure of the linear system. For convenience, we split the coefficient matrix into the element stiffness matrix  $R_i$  and the coupling to the other elements through the numerical flux integral  $F_i$ . The *exact* solution in  $E_i$  depends only on the upwind points of the bundle of streamlines passing through  $E_i$  and is independent of the solution elsewhere in the domain (Berre et al., 2005; Natvig et al., 2006). Using the upwind flux (5) preserves this one-side domain of dependence. In other words, the solution in  $E_i$  will only be influenced by elements that are intermediate neighbours in the upwind direction. Let  $U(i) = \{j \mid \mathbf{v} \cdot \mathbf{n} < 0 \text{ on } \partial E_i \cap E_j\}$  denote the indices of these elements. Then, if  $F_i^+$  denotes the flux *out of* element  $E_i$  and  $F_i^-$  the flux *into* element  $E_i$ , we have

$$-R_i T_i + F_i^+ T_i = B_i - F_i^- T_{U(i)}, \quad (7)$$

where  $T_{U(i)}$  are the degrees-of-freedom for all neighbouring elements of  $E_i$  in the upwind direction.

The key to obtaining a fast linear solver is to find an a priori reordering of the elements that renders the system of equations (7) in block-triangular form. In other words, we seek a reordering  $(p_1, \dots, p_N)$  of the  $N$  elements such that  $p_j < p_i$  if  $j \in U(i)$ , which means that it is possible to start at the inflow boundary and compute the solution element by element. Such a reordering can be found in  $N$  operators if it exists. If a reordering does not exist, there must be streamlines that pass through a grid cell more than once. If this occurs, the mutually connected elements must be solved for simultaneously. Nevertheless, the reordering still applies; the only difference is that we locally get a larger linear system associated with the interconnected elements; see (Natvig et al., 2006).

#### 4. NUMERICAL EXPERIMENTS

We now present numerical examples for two different test cases and discuss the dG approximations for computing time-of-flight in fractured porous media.

We consider two test cases. For both, we assume no-flow boundaries and an injector placed in the lower-left corner and a producer in the upper-right corner of the unit square  $\Omega = [0, 1] \times [0, 1]$ . The fractures are of permeability  $10^6$  D and are located in an otherwise homogeneous reservoir of permeability 1D as illustrated in Figure 2. The fracture width is set to 0.0001 length units. The velocity field  $\mathbf{v}$  is given such that the flux  $\mathbf{v} \cdot \mathbf{n}$  is constant over each element face.

We compare solutions obtained by the dG methods with a highly resolved streamline (SL) reference solution. We have also calculated a “reference” solution using the dG approximation of 7th order. For both reference solutions, we have used a grid consisting of  $320 \times 320$  standard matrix elements in addition to the elements that result from discretising the fractures with a resolution of eight elements in the direction across the fractures. The streamline solutions are obtained by back-tracking streamlines from the cell centre of each element.

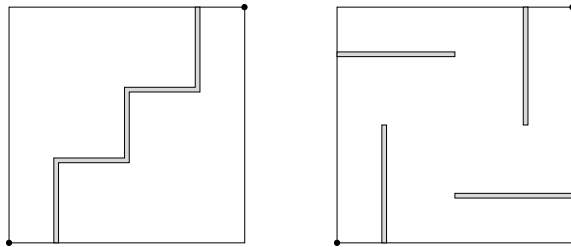


FIGURE 2. Fracture distribution in Case 1 (left) and Case 2 (right).

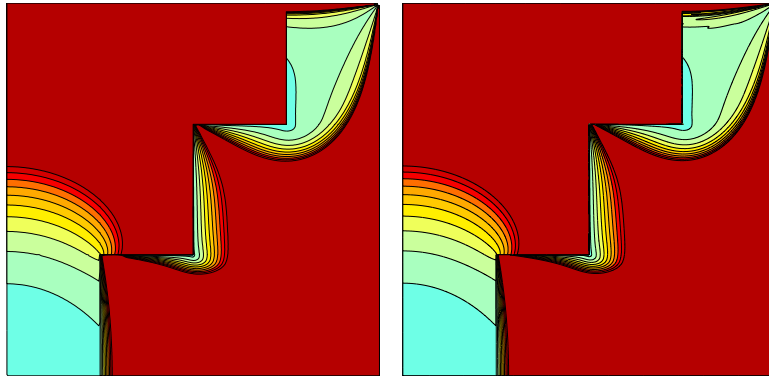
*Case 1.* In our first test case, a single fracture forms a staircase structure in the flow direction in an elsewhere homogeneous reservoir; see Figure 2. The reference solutions for this test case are shown in Figures 3(a) and 3(b). For all test examples, we have considered a second-order dG approximation.

Figure 3(c) displays the result of the dG approximation with order reduction across the fracture as described in Section 3.2. For this example, the fracture is resolved with one element in the direction across the fracture, thus reflecting the fact that the fracture initially is modelled as one-dimensional. As we can see, the breakthrough time at the production well is highly inaccurate. Figure 3(f) shows the result for the same test example, but without order reduction; that is, the same dG approximation is applied both for the matrix and the fracture elements and in this respect, the fractures are considered as fully two-dimensional. With this approximation, we observe instabilities in the solution, resulting in negative time-of-flights in some regions. On the other hand, the breakthrough-time is more correct than for the approximation displayed in Figure 3(c). To sum up, we see that we faced with two problems: either we get a highly erroneous breakthrough time at the producer, or we get negative values of time-of-flight.

Motivated by the fact that the transport is very rapid in the fractures, and our previous experience with dG methods for obstacle problems (Natvig et al., 2006), we try to increase the grid-resolution in the fractures. However, to avoid instabilities in the solution, we first consider examples where the order reduction of the dG approximation in the fracture elements is kept in the direction across the fracture. The results are depicted in Figures 3(d) and 3(e) for a resolution of four and eight elements across the fractures. Clearly, the results are significantly improved. In Figures 3(g) and 3(h), we display the results for refined fracture resolutions, but without order reduction of the dG approximation in the fractures. For eight elements across the fractures, we obtain a solution that resembles the SL reference solution, although one can still see small signs of instabilities.

*Case 2.* The fracture distribution in the second test case consists of four fractures in an elsewhere homogeneous reservoir as depicted in Figure 2. Figures 4(a) and 4(b) show the streamline reference solution and the solution obtained with the seventh-order dG method on a fine grid.

Figures 4(c) and 4(d) show results for a second and fourth-order dG approximation with order reduction and a resolution of eight elements across the fracture when order-reduction is applied. As we can see, the solutions are stable, but fail to completely capture the complex flow in the region near the upper-right fracture. Results for the same example,



(a) SL reference solution.

(b) dG reference solution.

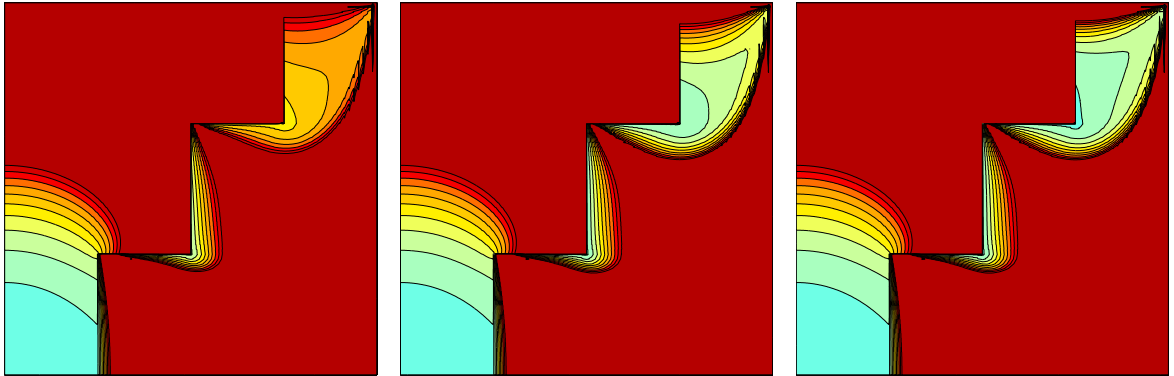
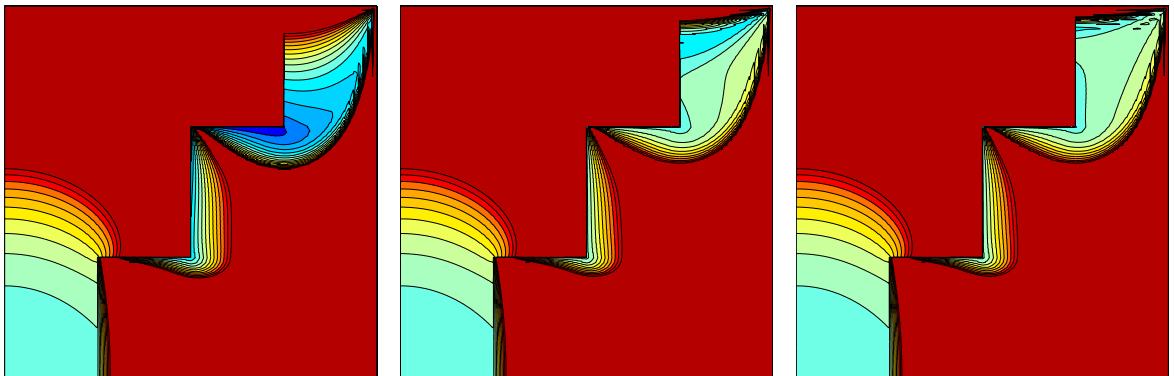
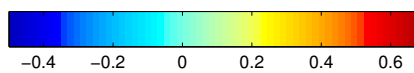
(c) Order red.,  $n_f = 1$ .(d) Order red.,  $n_f = 4$ .(e) Order red.,  $n_f = 8$ .(f) No order red.,  $n_f = 1$ .(g) No order red.,  $n_f = 4$ .(h) No order red.,  $n_f = 8$ .

FIGURE 3. Second-order dG approximations with  $80 \times 80$  standard matrix elements in addition to the elements that result from discretising the fracture by  $n_f$  elements in the fracture width, with and without order reduction.

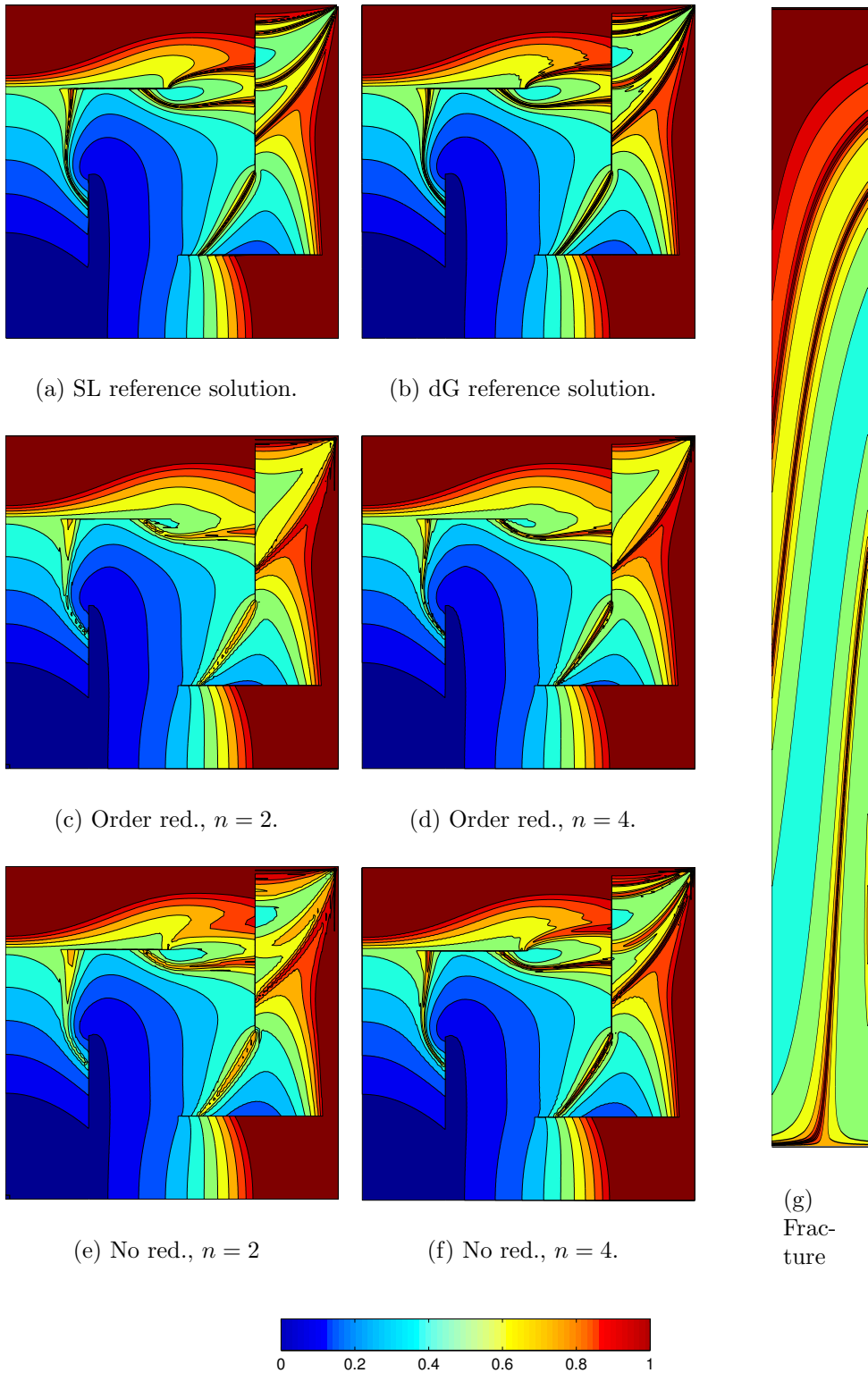


FIGURE 4. Second and fourth-order dG approximations with and without order reduction on a grid with  $80 \times 80$  standard matrix elements in the fracture width in addition to the elements that result from discretising the fracture by eight elements in the fracture width. The right plot shows the approximation with a subresolution of  $25 \times 25$  points in each element for the fracture from the upper-right part of the reservoir.

but without order reduction, are displayed in Figures 4(e) and 4(f). Here, the solutions are improved, but, as for Case 1, we can observe signs of instabilities in the solutions.

To further illustrate the necessity of a sufficient grid-resolution across the fractures, we have plotted the time-of-flight computed with the streamline simulator in the upper-right fracture element of Case 2 in Figure 4(g). This plot clearly demonstrates the complex flow pattern in the fracture.

## 5. CONCLUDING REMARKS

In this paper, we have investigated an efficient discontinuous Galerkin method for computing time-of-flight in fractured porous media. In particular, we have revealed the importance of a sufficient grid-resolution across the fractures. This is necessary since the time-of-flight is an integrated quantity that exhibits fine-scale details and contains large spatial variation within the fractures (even though these may have been modelled as lower-dimensional objects in the original grid model). To assure a stable solution, one can apply order reduction of the dG approximation in the direction across the fractures. This also results in a more efficient scheme due to a reduced number of unknowns for fracture elements.

A crucial part of the methodology is an optimal reordering of unknowns, which is based on prior information of the direction of flow. The result is an efficient method, which can be a grid-based alternative to streamline methods. Extension of the methodology to triangular and unstructured grids is currently in progress.

## REFERENCES

- Berre, I., K. H. Karlsen, K. -A. Lie, and J. R. Natvig (2005), Fast computation of arrival times in heterogeneous media, *Comput. Geosci.*, 9(4):179–201.
- Datta-Gupta A., and M. J. King (1995), A semianalytic approach to tracer flow modeling in heterogeneous permeable media, *Adv. Water Resour.*, 18(1).
- Natvig, J. R., and K.-A. Lie (2006), Fast computation of multiphase flow in porous media using discontinuous Galerkin and optimal ordering, preprint.
- Natvig, J. R., K.-A. Lie, B. Eikemo and I. Berre (2006), A discontinuous Galerkin method for computing single-phase flow in porous media, preprint.
- Prévost, M., M. G. Edwards, and M. J. Blunt (2002), Streamline tracing on curvilinear structured and unstructured grids, *SPE Journal*: 139–148.
- Reed, W. H., and T. R. Hill (1973), Triangular mesh methods for the neutron transport equation, *Tech. Report*, LA-UR-73-479, Los Alamos Sci. Lab.
- Hoteit, H., and A. Firoozabadi, Multicomponent fluid flow in discontinuous Galerkin and mixed methods in unfractured and fractured media, *Water Resour. Res.*, 41, W11412, doi:10.1029/2005WR004339.